World Electric Vehicle Journal

MDPI

Article

Suitable Growth Functions for the Electric Vehicle Market: A Retrospective Analysis of Forecast Quality

Theo Lieven

Institute for Mobility, University of St. Gallen, Blumenbergplatz 9, 9000 St. Gallen, Switzerland; theo.lieven@unisg.ch; Tel.: +41-79-957-9242

Highlights

- Logistic and Bass growth functions overpredict EV sales in a 12-year forecast; Weibull-type functions underpredict.
- Gompertz growth function is quite accurate and stable.
- The Gompertz function is recommended as the most suitable option.
- The Generalized Logistic function yields marginally better results but is less stable over time than the Gompertz function.

Abstract

While the adoption of electric vehicles can reduce CO_2 emissions, the extent of this reduction depends on the growth of the EV market. Sigmoid growth models, such as logistic or Gompertz function models, can be used to predict expected EV sales trends; however, their quality has not yet been comprehensively analyzed, as this would require looking into the future to compare today's predictions with future data. Since this is obviously not possible, this study takes a retrograde approach. It uses the available historical data to create forecasts that are then compared with the actual values from subsequent years. For example, a forecast based on data from 2010 to 2014 can be compared with the values achieved in years from 2015 to 2025. The quality of the functions is assessed using fit indices. Among the ten distinct functions tested, including two equivalent Gompertz functions, and under the stated saturation assumptions, the Gompertz family offers the most stable retrospective forecasts of EV stock (prediction period *MAPE* of 16.0% for the global data, against 15.1% for the generalized logistic, which performs comparably). The generalized logistic attains marginally better global point accuracy, whereas Gompertz is preferred for its greater stability across forecast origins and its more interpretable parameters.

Keywords: electric vehicle forecast; growth functions; retrospective forecast quality

Check for updates

Academic Editor: Joeri Van Mierlo

Received: 14 June 2026
Revised: 19 July 2026
Accepted: 21 July 2026
Published: 23 July 2026

Copyright: © 2026 by the author. Published by MDPI on behalf of the World Electric Vehicle Association. Licensee MDPI, Basel, Switzerland. This article is an open access article distributed under the terms and conditions of the Creative Commons Attribution (CC BY) license.

1. Conceptual Formulation

In line with SDG 7 of the United Nations' Sustainable Development Goals, more consumers are opting for electric vehicles (EVs) as a clean, efficient, and practical mode of transportation [1], with annual sales worldwide growing steadily since they were first introduced in 2010 [2]. It is thus important for decision-makers to have reliable forecasts of how this trend will continue: politicians want to know whether electric mobility can help achieve the zero-carbon target for passenger transport by 2050 [3,4], and industry leaders want to prepare for future demand. In addition, knowledge of expected sales is of interest

when comparing periods with and without government subsidies, and conclusions can be drawn about market growth, infrastructure, and policy needs [5,6].

The first attempts to predict future EV sales were made as early as 2010, but at that time, due to the lack of historical data, stated-preference methods were used [7]. Over time, methods were developed to estimate the market share of EVs in the overall market using ordinary least squares regression (OLS), with numerous factors as predictors, including government subsidies [8]. As the amount of historical data increased, these methods were adapted to different models. Srinivasan (2025) [9] used the autoregressive integrated moving average (ARIMA) and long short-term memory (LSTM) models with historical EV sales data from 2010 to 2023, with mixed prediction quality. While global sales in 2025 totaled 21.621 million EVs [2], the ARIMA and LSTM models predicted 103.226 million and 6.960 million, respectively.

The historical EV market data show exponential rather than linear growth, suggesting that a linear function cannot adequately represent the data. The shape of exponential growth functions can vary considerably. The simplest case is when the relative growth rate is constant: $\boldsymbol{f'(x)/f(x) = b}$. However, there are also super- and sub-exponential growth patterns. The researcher's task is to define the function that best represents the market data. This is not easy at the beginning of a growth cycle: after the initial "lag", i.e., starting at 0, and a few measurement points, it can only be discerned that the growth is exponential. Malthus (1789) [10] hypothesized that growth continues indefinitely; however, experience shows that after accelerating growth, a decelerating phase begins after an inflection point until a saturation level is reached. This makes it difficult for time-series or machine learning models to predict the subsequent trajectory at the beginning of a growth period. They lack the theoretical foundation for identifying an inflection point and the asymptotic approach towards the saturation level, because this development is unpredictable in the initial phase. This is why this study focuses solely on S-shaped sigmoidal models.

It could be argued that these growth functions are descriptive because they depend on time; although this might be causally unsatisfactory, because it is not time that affects growth, but rather a state of the system (initially, an increasing number of customer referrals; later, a saturated market). However, for the Gompertz function it is possible to transform the time-dependent function $N(t) = K \cdot e^{-b \cdot e^{-\alpha \cdot t}}$ to a time-independent differential equation $\frac{dN}{dt} = \propto \cdot N \cdot ln\left(\frac{K}{N}\right)$ (with a as the decay rate of growth potential, K as the saturation limit, and N as the actual stock). This is the so-called autonomous Gompertz differential equation, which can serve as a theoretical foundation. Thus, sigmoid growth models can be seen as theory-driven, like resource availability in the logistic function and innovation and imitation in the Bass model.

Rietmann et al. (2020) [11] used a sigmoid function, in the form of logistic growth, to predict sales figures across 26 countries based on historical data up to 2018. The 2025 predictions were unsatisfactory from today's perspective, as they were more than two-thirds higher than the actual sales data.

To the best of our knowledge, there is no comprehensive analysis regarding which sigmoid growth functions should be used in specific application areas. There has been no investigation into which function best describes the electric vehicle market. Here, "best" refers not only to a specific point in time but also to the stability of predictions across successive data collection periods. Predictions change over time (e.g., due to external shocks or government incentives); however, it would be advantageous to have a function that does not deviate excessively from previous results with each new calculation—thereby keeping prediction variance to a minimum. The aim of this study is to determine which growth function best approximates this ideal for the EV market, answering the following research questions:

- Which sigmoid growth functions provide the most accurate out-of-sample forecasts of cumulative EV adoption?
- Does model performance differ between a global aggregate and a policy-sensitive national market?
- How sensitive are rankings to the assumed saturation level and forecast horizon?

We take a retrograde approach, comparing predictions made based on earlier data to actual sales figures. Since the EV sales figures (and thus the total inventories (In this study, the EV stock is calculated as cumulative sales. Scrappings are not considered until 2025, as only 1.2% of EVs will have been scrapped over the entire period from 2010 to 2025)) from 2010 to 2025 are known, previous predictions can be evaluated as if at the end of a former year. Starting at the end of 2014, we treat the subsequent figures as unknown and predict them using one of the growth functions under test; this is repeated for each subsequent year up to the end of 2025. From the end of 2014 to the end of 2025, there are 12 predictions to compare with the actual results. Relevant fit indices are used to determine the most suitable growth functions for the EV market.

The next section explains the theory of sigmoids based on the existing literature. The ten different growth functions, including two equivalent Gompertz functions, are then adjusted to historical data from 2010 to 2025. One dataset covers global sales; the other, from Germany, is included to analyze the effects of several incentive changes that led to sharp fluctuations until the purchase subsidy was suddenly eliminated in December 2023.

2. Literature Review and Theory

Growth can be described as an increase in size over time [12]. Growth functions are applied to many areas in the natural and social sciences; Table 1 presents an overview.

To better understand the features of sigmoid growth functions, an idealized representation based on acceleration, speed, and distance is shown in Figure 1.

The term growth is used to describe both the increase per unit of time and the cumulative size. The latter is the distribution function; the former is the first derivative of this function, or the density function. The distribution function f usually starts at zero and approaches a maximum, the so-called saturation level, asymptotically. The density function f' (first derivative) describes the rate of growth, symbolically, "speed". The inflection point lies between the beginning and the end. Before this point, growth is progressive due to positive acceleration, which is represented by the second derivative. At the root of f'', the maximum speed is reached at the inflection point, and from there growth is degressive (i.e., the speed decreases until it asymptotically comes to a standstill, where the saturation level is reached). Every growth process must be set in motion. The maximum of this initiation is reached at the maximum acceleration point in the second derivative f'' (at a root of the third derivative f'''). The maximum of the third derivative f''' at the root of the fourth derivative f'''' could be symbolically described as "full throttle".

The three most important points for the shape of the growth function are the saturation level, the position of the inflection point on the x-axis, and the function's slope. Many growth functions are defined by only these three parameters, while some have a fourth parameter that allows for a more flexible definition of the inflection point.

The best-known of these sigmoid functions is the logistic growth function [30,31]. The inflection point is located at half of the saturation level. Around this inflection point, the function is point-symmetric (i.e., a 180° rotation around the inflection point produces the same image). The inflection point being reached exactly halfway through the curve is a significant limitation; some growth processes may follow a different pattern, meaning that the inflection point is reached either earlier or later. One function that describes such growth is the Gompertz growth function, which was developed before the logistic function [29]. In

this function the inflection point occurs before the halfway point; the cumulative growth is not half the saturation level but rather the saturation level divided by e (i.e., approximately 36.8% of the saturation). Other functions use a special parameter that flexibly represents the inflection point [32,33].

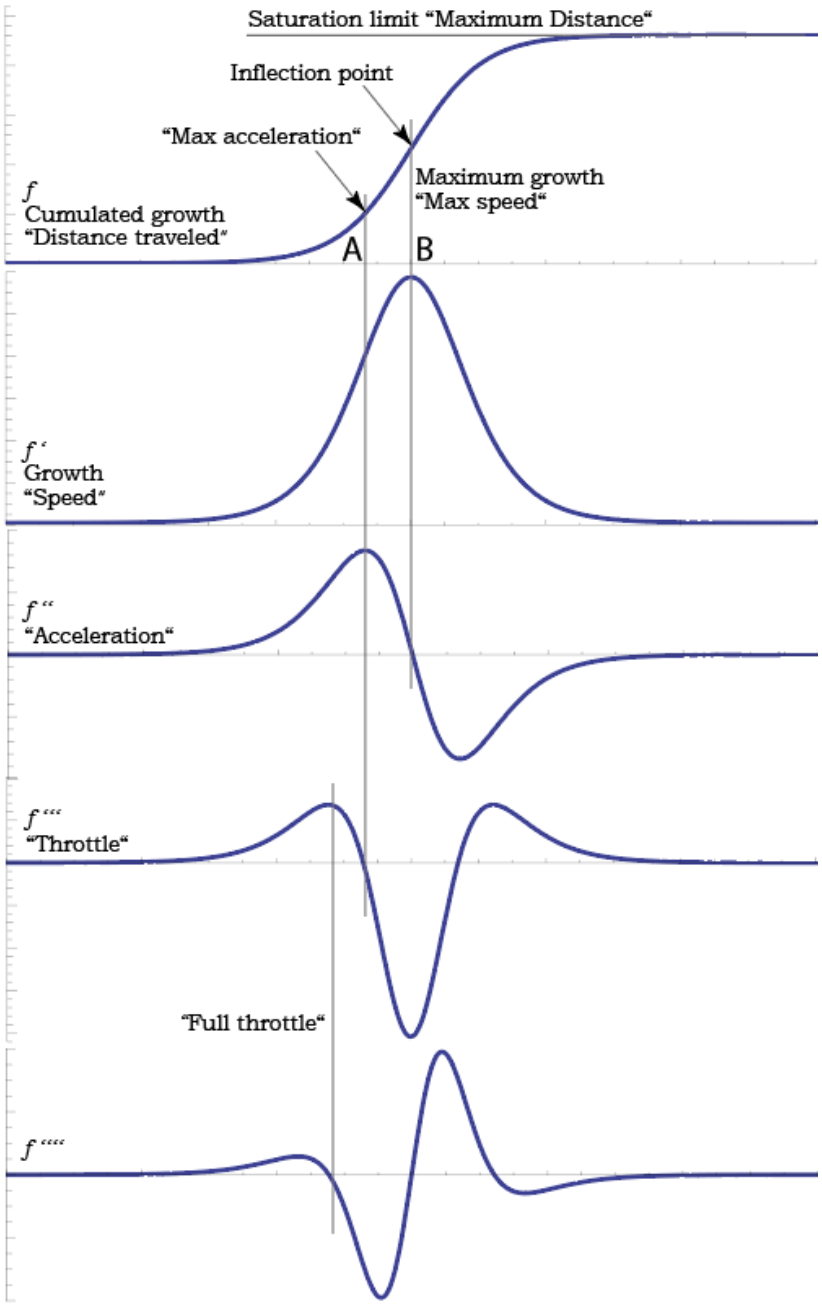


Figure 1. Growth function with four derivatives.

The reason for the large number of different growth functions is their application across a wide range of areas; every growth process is different, and scientists seek the most suitable model. Many comparative studies have attempted to find the optimal model for a particular application. Tjørve and Tjørve (2017) [34] analyzed several kinds of Gompertz functions. Young (1993) [35] compared nine diffusion models and concluded that the Bass model was superior to others when the saturation limit was unknown; the data used did not relate to a specific area of application but were taken from the existing literature. Zeide (1993) [12] compared 12 growth models for plant growth. Buchanan et al. (1997) [36] compared several growth models that predict bacterial growth.

Table 1. Literature studies. References [12–29].

Study	Field/Application Context	Dependent Variable/Phenomenon	Model/Equation	Forecasting Horizon/Dynamic Property	Evaluation/Analytical Basis	Main Findings/Contribution
[12] Zeide (1993), Forest Science	Forestry/mensuration: theoretical review of growth equations	Tree and stand size (height, diameter, volume) over time	Comparative analysis of sigmoidal growth equations (Gompertz, logistic, monomolecular/Mitscherlich, Chapman–Richards, Weibull); decomposition of the growth rate	Full ontogenetic (lifetime) trajectory; sigmoidal with an inflection point	Analytical classification by biological interpretability; fit to growth data	Splits the growth rate into two opposing components: intrinsic multiplicative expansion and a constraining decline term. Distinguishes empirical from theoretically grounded equations and favors those with biologically meaningful parameters.
[13] Goriely (2017), Springer (book)	Biomechanics/applied mathematics: morpho elasticity	Volumetric and morphological growth of soft tissue; shape and residual stress	Continuum-mechanics framework; multiplicative decomposition of the deformation gradient F = A·G (elastic × growth)	Continuous developmental time; steady and evolving configurations	Analytical/mechanical consistency; stability analysis; residual stress predictions	Provides a rigorous continuum theory linking growth to mechanical stress and instabilities (buckling, wrinkling, pattern formation); shows residual stress arises from incompatible growth.
[14] Monod (1949), Annu. Rev. Microbiol.	Microbiology: bacterial batch culture	Specific growth rate/biomass as a function of limiting nutrient	Monod equation: $\mu = \mu_{max} \cdot S/(K_s + S)$	Exponential (log) phase within the batch cycle (lag → exponential → stationary)	Empirical fit to culture data; hyperbolic (saturation) kinetics	Growth rate is a saturating function of substrate concentration; defines growth yield and saturation constant. Foundational for microbial kinetics and chemostat theory.
[15] West, Brown & Enquist (1997), Science	Biology/metabolic ecology: cross-taxa	Metabolic and other biological rates vs. body mass (allometry)	Fractal-like, space-filling, hierarchical branching resource-distribution network model	Not temporal; a cross-species steady-state scaling relationship	Derives exponents as multiples of ¼; compared with observed allometric exponents	Explains ubiquitous quarter-power scaling (metabolic rate $\propto M^{3/4}$) from optimized branching transport networks; gives a mechanistic basis for allometry and later ontogenetic growth models.

Table 1. *Cont.*

Study	Field/Application Context	Dependent Variable/Phenomenon	Model/Equation	Forecasting Horizon/Dynamic Property	Evaluation/Analytical Basis	Main Findings/Contribution
[16] Murray (2002), Mathematical Biology I (book)	Mathematical biology: single-species/temporal dynamics	Population size, reaction kinetics, temporal dynamics	ODE models: logistic, delay/discrete logistic, interacting populations, enzyme kinetics	Continuous time; equilibria and long-term dynamics	Stability and bifurcation analysis; phase-plane methods	Canonical reference deriving and analyzing deterministic growth and interaction models; establishes stability, oscillation, and threshold behavior.
[17] Murray (2003), Mathematical Biology II (book)	Mathematical biology: spatial and biomedical models	Spatial spread, pattern formation, wave propagation	Reaction–diffusion systems; Turing patterns; traveling waves (Fisher–KPP)	Space–time; asymptotic wave speeds and patterns	Linear stability analysis; traveling-wave existence and speed	Extends growth modeling to space; shows diffusion-driven instability generates biological patterns and invasion fronts.
[18] Hunt (1982), Edward Arnold (book)	Plant physiology/crop science	Plant dry mass and size over time (growth analysis)	Functional (curve-fitting) approach: polynomials, splines, and classic growth functions, yielding derived indices (RGR, NAR)	Discrete harvest series across a growing season	Goodness-of-fit; smoothed derivatives (relative growth rate)	Advocates fitting continuous functions to harvest data to derive instantaneous growth indices, superseding the classical interval approach.
[19] Hunt (1990), Unwin Hyman (book)	Plant physiology: introductory/methodological	Plant growth (dry weight, leaf area)	Classical growth analysis: RGR, unit leaf rate, leaf area ratio; exponential/logistic fitting	Sequential harvests across development	Interval formulae and fitted-curve derivatives	Accessible primer standardizing plant growth-analysis indices and their calculation.
[20] Evans (1972), Univ. of California Press (book)	Plant physiology: comprehensive treatise	Plant growth quantified (mass, area, allocation)	Classical plant growth-analysis framework (RGR, NAR/ULR, LAR) with statistical treatment	Longitudinal harvest sequences	Statistical estimation of growth parameters and their errors	Definitive foundational text formalizing quantitative plant growth analysis and its experimental/statistical basis.

Table 1. *Cont.*

Study	Field/Application Context	Dependent Variable/Phenomenon	Model/Equation	Forecasting Horizon/Dynamic Property	Evaluation/Analytical Basis	Main Findings/Contribution
[21] Kermack & McKendrick (1927), Proc. R. Soc. A	Epidemiology: theoretical	Numbers of susceptible/infected/removed over an epidemic	SIR compartmental ODE model with mass-action transmission	A single epidemic wave (outbreak duration)	Analytical threshold theorem; final epidemic size relation	Introduces the SIR model and the threshold (reproduction) condition—an epidemic occurs only above a threshold condition involving the basic reproduction threshold—and derives the final epidemic size.
[22] Keeling & Rohani (2008), Princeton Univ. Press (book)	Epidemiology/disease ecology	Infection prevalence and incidence dynamics	Compartmental (SIR/SEIR), stochastic, network, spatial, and age-structured models	Short-term outbreaks through to long-term endemic dynamics	Analytical plus simulation; R_0 estimation; model comparison	Comprehensive modern reference synthesizing deterministic and stochastic epidemic models and their parameterization.
[23] Viboud, Simonsen & Chowell (2016), Epidemics	Epidemiology: early outbreak phase; 20+ historical outbreak datasets	Cumulative/incident case counts in the early ascending phase	Generalized growth model (GGM): $C'(t) = r \cdot C(t)^P$, with scaling parameter $p \in [0, 1]$	Early ascending phase (first generations); short term	Fit to 20+ historical outbreaks; estimation of p; captures sub-exponential growth	Many real outbreaks grow sub-exponentially ($p < 1$); the flexible GGM improves early-phase characterization and short-term forecasts versus assuming pure exponential growth.
[24] Laird (1964), Br. J. Cancer	Oncology/tumor biology: experimental animal and human tumor data	Tumor volume/mass over time	Gompertz growth function fitted to tumor data	Full tumor growth course toward an asymptote/plateau	Empirical fit quality across many tumors; parameter consistency	Demonstrated that many experimental tumors are well described by a Gompertz curve—exponential growth with a continuously decelerating specific growth rate; the retardation constant characterizes tumors.

Table 1. *Cont.*

Study	Field/Application Context	Dependent Variable/Phenomenon	Model/Equation	Forecasting Horizon/Dynamic Property	Evaluation/Analytical Basis	Main Findings/Contribution
[25] Solow (1956), Q. J. Econ.	Macroeconomics: theoretical	Output and capital per worker over time; long-run growth	Neoclassical growth model: production function with substitutable capital and labor; capital accumulation ODE	Long-run transition to a steady state	Analytical stability of the steady state; comparative statics	The economy converges to a stable steady-state capital–labor ratio; sustained per capita growth requires exogenous technical progress, not capital accumulation alone.
[26] Swan (1956), Economic Record	Macroeconomics: theoretical	Capital accumulation and output growth	Neoclassical (Solow–Swan) growth model, Cobb–Douglas technology	Long-run steady state	Analytical/diagrammatic (Swan diagram) equilibrium analysis	Independently derives the neoclassical growth framework; diminishing returns drive convergence to a steady state, complementing Solow.
[27] Barro & Sala-i-Martin (1995), McGraw-Hill (book)	Macroeconomics: graduate text with cross-country evidence	Long-run growth and cross-economy convergence	Neoclassical (Solow–Ramsey) plus endogenous growth models; empirical convergence regressions	Long-run; multi-decade cross-country panels	β- and σ-convergence; growth regressions	Consolidates growth theory and evidence; documents conditional convergence (~2%/yr) and the role of technology and human capital.
[28] Mankiw, Romer & Weil (1992), Q. J. Econ.	Macroeconomics: empirical; ~98 non-oil countries	Cross-country differences in income per capita and growth	Augmented Solow model adding human capital; cross-country OLS regressions	Long-run/steady state (1960–1985), cross-sectional	Regression fit (R^2); test of predicted factor-share coefficients; conditional convergence	The augmented Solow model with human capital explains roughly 75–80% of cross-country income variation and supports conditional convergence; savings and population growth affect income as theory predicts.
[29] Gompertz (1825), Phil. Trans. R. Soc. London	Actuarial science/demography: human mortality tables	Age-specific mortality (force of mortality)/survivorship	Gompertz law: mortality rises exponentially with age, $\mu(x) = B \cdot e^{cx}$	Adult lifespan/age progression	Fit to life-table mortality data	Establishes that adult death rates rise geometrically with age; the Gompertz distribution function later became a foundational sigmoidal growth model across biology.

Of particular interest in this study are forecasts of EV sales using common growth functions. Huo and Wang (2012) [37] used the Gompertz, logistic, and Richards functions to analyze vehicle stock in China, while Brdulak et al. (2021) [38] analyzed the market diffusion of innovative EV technology in Europe using the Bass growth model. Of note is the inflection point, when cumulative growth transitions from convex to concave, and the point in time when, according to Rogers' (2003) [39] diffusion theory, the sales market transitions from innovators and early adopters to the early majority phase, at which point the product becomes mainstream. The assumption of the existence of such a point is adopted in this study by the moment of maximum acceleration (Figure 1).

In further work, Fan et al. (2025) [40] evaluated the Chinese EV market using a Bass model, accounting for policy measures; Turkey, Alatawneh and Ghunaim (2024) [41] predicted EV ownership using the Gompertz function; Ayyadi and Maaroufi (2018) [42] aimed to predict the diffusion of EVs in Morocco by applying the logistic, Gompertz, and Bass models; Dalkic-Melek et al. (2025) [43] used the Gompertz and logistic growth functions regarding the motorization rate and economic growth in Turkey; and Tang et al. (2013) [44] modeled CO_2 emissions and energy savings using a logistic model.

Kumar et al. (2022) [45] compared four growth functions by adjusting them to EV sales data from 20 countries between 2011 and 2018. They recommended an appropriate growth model based on the goodness-of-fit indices from the historical period. It was not possible for them to verify how well the models matched the actual sales figures from 2019 onwards because these were not available at the time.

This study aims to compare the goodness of fit in the forecast period. This is achieved by looking back and making a prediction from a particular year using only data up to the end of that year and then comparing this forecast with the actual sales figures.

3. Data, Method, and Procedure

3.1. Data

Significant EV sales began in 2010. In the same year, Victor Irle from Sweden began compiling sales figures from different countries and publishing them as EV Volumes [2]. This has now grown into a comprehensive global database characterized by its consistent data (The official figures for Germany (Kraftfahrt-Bundesamt [KBA] Germany, 2026) [46] could not be used because EV sales have only been reported since 2017. In addition, the vehicle types changed in the meantime. For Germany, the KBA data are often 1 to 3% lower because the KBA reports early, around the 8th of the following month, while EV Volumes collects data until the end of the following month), and is now part of the automotive consulting firm J.D. Power. In this study, we used data from 2010 to the end of 2025 and fitted growth functions to them. The worldwide growth curve appears to continue increasing exponentially. In Germany, sales rose sharply from 2020 to 2022 due to government subsidies but then fell from 2023 onwards after the subsidy was reduced and the incentive program was suddenly terminated. Thus, the inventory curve from accumulated sales is linear rather than exponential (Figure 2). To compare the appropriateness of the growth functions, Germany was included in the analyses.

3.2. Method

Ten different growth functions, including two equivalent Gompertz functions, were fitted to the historical data. The suitability of the functions was determined by using fit indices, which consider the differences between the actual figures and those predicted by the model.

The first fit index used was the root mean square error (*RMSE*), which is determined by the root of the average of the squared errors between the actual and predicted values:

$$RMSE = \sqrt{\frac{1}{n}\sum_{i=1}^{n}(actual\ value_i - predicted\ value_i)^2} \quad (1)$$

where n is the number of observations (years). The *RMSE* indicates how much the model's predicted values deviate from the actual values on average; smaller values indicate a better fit.



Figure 2. Accumulated EV (BEVs and PHEVs) sales worldwide (When this study uses the terms "world" or "worldwide," they refer to the countries where EV sales were recorded. In fact, these countries represent only 85% of the world's population. Where possible, the term was replaced by "global") and in Germany, 2010–2025.

The next measure of quality used was the Akaike information criterion (*AIC*):

$$AIC = 2k - 2\ln(L) \quad (2)$$

where k is the number of estimated parameters in the model and ln(L) is the log-likelihood, which indicates how well the model explains the data. This likelihood is defined as

$$\ln(L) = -\frac{n}{2}\left[\ln(2\pi) + \ln\left(\frac{1}{n}\sum_{i=1}^{n}(actual\ value_i - predicted\ value_i)^2\right) + 1\right] \quad (3)$$

Again, the mean squared error is used. However, by accounting for the number of model parameters, the *AIC* measures the trade-off between model quality and complexity. The smaller the *AIC*, the better the model.

The third fit index used was the mean absolute percentage error (*MAPE*),

$$MAPE = \frac{100\%}{n}\sum_{i=1}^{n}\left|\frac{actual\ value_i - predicted\ value_i}{actual\ value_i}\right| \quad (4)$$

which shows the average prediction error as a percentage. According to Lewis (1982) [47], a *MAPE* of $\leq$10% has high forecasting accuracy, 10–20% is good, 20–50% is feasible, and a *MAPE* of $\geq$50% denotes low accuracy.

Since *MAPE* deviations are expressed as percentages, data scaling does not affect comparability, unlike *RMSE*, where, for example, an *RMSE* of 5 may be a good value for vehicle prices but it is rather poor for test scores. Since the adjustments are made to two datasets that are completely different in magnitude (globally, the EV stock at the end of 2025 was over 80 million, while in Germany it was only 4.4 million), the *MAPE* seems to be the more reliable measure for assessing the quality of the forecast, at least for the purposes of this study.

Another quality criterion that can be considered is the range of predictions over time. Predictions change over the years; both researchers and practitioners want the growth curves to follow a pattern that is as similar as possible, so that new predictions do not deviate too much from older ones. The standard deviation of the inflection points is calculated as a measure of this dispersion.

The method used to compare these indices had two stages. First, the indices were calculated for the period during which the function parameters were determined using historical data (adaptation quality). Second, the prediction quality was assessed using fit indices for subsequent years. For the end of 2014, the parameters for the growth function were calculated using data from 2010, 2011, 2012, 2013, and 2014, thereby optimally adjusting the function to the data available up to that point. The corresponding function with these parameters was then used to calculate the figures for 2015–2025. Since the actual sales figures for that period are known, the quality of the prediction could be assessed. This procedure was repeated for all subsequent years.

3.3. Procedure

Two datasets from EV Volumes (2026) [2] were used: the aggregated EV (including both battery electric vehicles (BEVs) and plug-in hybrid vehicles (PHEVs)) sales worldwide and in Germany from 2010 until the end of 2025 (Table 2) (The figures were calculated by adding up sales. Scrappage was not considered. Due to low sales figures in the early years, this was unlikely to have a significant impact. (According to a calculation with a Weibull function, until 2025, only 1.2% of EVs were scrapped in total.)).

Table 2. Sales and accumulated sales globally and in Germany from 2010 to 2025.

Year	Sales World (Thsds.)	Inventory World (Thsds.)	Sales Germany (Thsds.)	Inventory Germany (Thsds.)
2010	6.455	6.455	0.144	0.144
2011	50.660	57.115	1.862	2.006
2012	132.276	189.391	6.288	8.294
2013	209.923	399.314	6.714	15.008
2014	323.797	723.111	13.280	28.288
2015	546.984	1270.095	24.220	52.508
2016	797.637	2067.732	28.109	80.617
2017	1270.451	3338.183	58.363	138.980
2018	2089.995	5428.178	72.588	211.568
2019	2286.784	7714.962	112.847	324.415
2020	3258.637	10,973.599	400.466	724.881
2021	6802.977	17,776.576	690.640	1415.521
2022	10,563.144	28,339.720	842.799	2258.320
2023	14,211.596	42,551.316	714.332	2972.652
2024	17,800.052	60,351.368	583.872	3556.524
2025	21,621.232	81,972.600	885.602	4442.126

Note: Sales include both BEVs and PHEVs.

Ten growth functions, including two equivalent Gompertz functions, were examined in this study (Table 3). The two Gompertz functions are equivalent and yield the same results (Modified Gompertz = $M \cdot e^{-e^{-\frac{t-\beta}{\gamma}}} = M \cdot e^{-e^{\frac{\beta}{\gamma}} \cdot e^{-\frac{t}{\gamma}}}$. Set $e^{\frac{\beta}{\gamma}} = b$, $\frac{1}{\gamma} = c \Rightarrow M \cdot e^{-b \cdot e^{-c \cdot t}}$, which is the original Gompertz function). However, the parameters of the modified Gompertz functions are easier to interpret. The inflection point is determined solely by β, and the point of maximum acceleration is calculated as the sum of β and β multiplied by a scalar.

Starting at the end of 2014, the growth functions' parameters were determined by adapting them to the data from 2010 to 2014 using the nonlinear regression function in SPSS (Version 31) with the least squares method. Values of 2 billion vehicles worldwide (=2,000,000 Thsd.) and 45 million in Germany were set as the saturation levels for all

functions. The maximum capacity for passenger cars has been estimated to be between 1.5 and 3 billion [48]. The saturation level could not be reliably identified when there were fewer than five observations: attempts to estimate it at the earliest forecast origins produced non-convergence or economically implausible estimates, which is precisely why it is fixed from external sources (total vehicle fleet projections) (A sensitivity analysis, using assumed saturation levels of 1.5 bn, 2 bn, and 3 bn, shows that the results are not affected).

The time variable t started at 1 in 2010. Thus, the Gompertz function for the global data at the end of 2014 was

$$2{,}000{,}000 \cdot e^{-11.885 \cdot e^{-0.081405 \cdot t}} \quad (5)$$

The results for this function are shown in Table 4.

Table 3. Growth functions used in this study.

	Distribution Function	Parameters	Max Acceleration Point (Root of 3rd Derivation)	Inflection Point (Root of 2nd Derivation)
[49] Weibull (1951)	$M \cdot \left(1 - e^{-\left(\frac{t}{\lambda}\right)^k}\right)$	M: Saturation limit l > 0: Scale parameter k > 0: Form parameter	$\lambda\left(\frac{3(k-1)-\sqrt{(k-1)(5k-1)}}{2k}\right)^{1/k}$	$\lambda\left(\frac{k-1}{k}\right)^{1/k}$
[50] Janoschek (1957)	$M - (M - y_0) \cdot e^{-ct^m}$	M: Saturation limit y_o: Starting value at t = 0 m: Shape parameter	$\left(\frac{3(m-1)-\sqrt{(m-1)(5m-1)}}{2mc}\right)^{1/m}$	$\left(\frac{m-1}{c \cdot m}\right)^{1/m}$
Morgan–Mercer–Flodin [51] Morgan et al. (1975)	$M \cdot \frac{t^d}{b+t^d}$	M: Saturation limit b: Scale along t d: Shape	$\left(\frac{b\left(2(d-1)(d+1)-d\sqrt{3(d-1)(d+1)}\right)}{(d+1)(d+2)}\right)^{1/d}$	$\left(b \cdot \frac{d-1}{d+1}\right)^{1/d}$
Chapman–Richards [32] Richards (1959)	$M \cdot \left(1 - e^{-k \cdot t}\right)^m$	M: Saturation limit k: Growth rate m: Shape	$\frac{1}{k} ln\left(\frac{3m-1-\sqrt{5m^2-6m+1}}{2}\right)$	$\frac{\ln(m)}{k}$
Levakovic I [52] Levakovic (1935)	$M \cdot \left(\frac{t^d}{t^d+b}\right)^c$	M: Saturation limit b: Horizontal position c: Shape d: Asymmetry parameter	$\left(\frac{b\left((d+1)(3cd+d-4)-d\sqrt{(c+1)(d+1)(5cd+c+d-7)}\right)}{2(d+1)(d+2)}\right)^{1/d}$	$\left(\frac{b(cd-1)}{d+1}\right)^{1/d}$
[53] Bass (1969)	$M \cdot \frac{1-e^{-(p+q)\cdot t}}{1+\frac{q}{p} \cdot e^{-(p+q)\cdot t}}$	M: Saturation limit p: Coefficient of innovation q: Coefficient of imitation	$\frac{ln\left(\frac{2q-\sqrt{3}\cdot q}{p}\right)}{q+p}$	$\frac{ln\left(\frac{q}{p}\right)}{q+p}$
Logistic [30] Verhulst (1838)	$\frac{M}{1+ae^{-rt}}$	M: Saturation limit r: Growth rate a: Constant	$\frac{ln\left(2a-\sqrt{3}\cdot a\right)}{r}$	$\frac{ln(a)}{r}$
Generalized logistic [54] Tsoularis and Wallace (2002)	$\frac{M}{\left(1+a \cdot e^{-r \cdot t}\right)^{1/v}}$	M: Saturation limit a: Changes horizontal position r: Growth rate n: Asymmetry parameter	$\frac{ln\left(-\frac{a\sqrt{v^2+6v+5}}{2v}+\frac{3a}{2v}+\frac{a}{2}\right)}{r}$	$\frac{\ln\left(\frac{a}{v}\right)}{r}$
[29] Gompertz (1825)	$M \cdot e^{-b \cdot e^{-c \cdot t}}$	M: Saturation limit b: Changes horizontal position c: Growth rate	$\frac{ln\left(\frac{(3-\sqrt{5})b}{2}\right)}{c}$	$\frac{\ln(b)}{c}$
Modified Gompertz [55] Dargay et al. (2007)	$M \cdot e^{-e^{-\frac{t-\beta}{\gamma}}}$	M: Saturation limit b: Inflection point g: Time scaling	$ln\left(\frac{3}{2}-\frac{\sqrt{5}}{2}\right) \cdot \gamma + \beta = -0.96242365 \cdot \gamma + \beta$	b

The same procedure was followed for the end of each of the subsequent 11 years. The fit indices were determined separately for the adaptation and prediction periods.

Table 4. Actual inventories and forecasts based on historic data until 2014 calculated using (5) (As can be seen from Table 4 for 2010 and 2011, the small actual inventory figures led to large percentage errors (for 2010: $|35 - 6|/6 = 441\%$). To assess the quality of the forecast, the *MAPE* values for the first two years were therefore not considered in the following [56]).

	Adaptation Period									Prediction Period						
Year	**2010**	**2011**	**2012**	**2013**	**2014**	**2015**	**2016**	**2017**	**2018**	**2019**	**2020**	**2021**	**2022**	**2023**	**2024**	**2025**
Actual Inventory	6	57	189	399	723	1270	2068	3338	5428	7715	10,974	17,777	28,340	42,551	60,351	81,973
Forecast	35	82	181	375	734	1361	2408	4072	6611	10,332	15,595	22,792	32,338	44,643	60,097	79,042
Absolute percentage error	441%	44%	4%	6%	1%	7%	16%	22%	22%	34%	42%	28%	14%	5%	0%	4%

Note: $t = 1$ for 2010; inventories in Thsds; absolute percentage error = Abs(Forecast–Actual)/Actual.

The sums of all absolute percentage errors were divided by n observations. The n values used to calculate the mean were obtained in the adaptation period as $n_{\text{adaption}} = 3 + 4 + 5 + \ldots + 14 = 102$ (note that the first two years were disregarded), and for the prediction period as $n_{\text{prediction}} = 11 + 10 + 9 + \ldots + 2 + 1 = 66$ (A supplemental spreadsheet is available for better understanding). The sum in the adaptation period was 1787%, resulting in an average (102) of 17.52%, representing the *MAPE*. For the prediction period, this *MAPE* was 1056% ÷ 66 = 16.00%. The *RMSE* and *AIC* were calculated similarly. The same procedure was applied to all the other growth functions for both the global and German figures.

4. Results

4.1. Three Clusters of Growth Functions

Researchers and practitioners alike prefer not to see overly large jumps in recurring predictions. A measure of the consistency of the predictions is the standard deviation (SD) of the inflection point. A comparison of the SDs resulted in three clusters (Table 5):

Table 5. Standard deviations of the inflection points.

	Function	Std. Dev. World	Std. Dev. Germany
Cluster 1	Weibull	17.380	15.681
	Janoschek	18.029	16.389
	Morgan–Mercer–Flodin	14.810	13.460
	Chapman–Richards	19.495	17.663
	Levakovic I	14.715	13.865
Cluster 2	Bass	2.070	1.832
	Logistic	2.493	1.999
Cluster 3	Generalized Logistic	3.696	4.391
	Gompertz	2.465	4.223
	Modified Gompertz	2.465	4.223

To verify the three-cluster distribution, a k-means analysis was performed using the years of the inflection points. The result confirmed the distributions for both the global and German data, as shown in Table 5.

Not surprisingly, the adjustments using historical data from 2010 through the end of 2025 were the most accurate. All predicted the actual values of approximately 82 million vehicles worldwide and 4.5 million in Germany for 2025 with reasonable accuracy (graphs at the right end of Figures 3 and 4).

Using the figures in cluster 1 from the end of 2014, these functions predicted 2025 numbers that were far too low (globally, around 15 million EVs). These were the Weibull, Janoschek, Morgan–Mercer–Flodin, Chapman–Richards, and Levakovic I functions. At the end of 2014, cluster 2 functions predicted a far too high stock level for 2025 (globally, nearly 1 billion, in Germany, about 20 million).

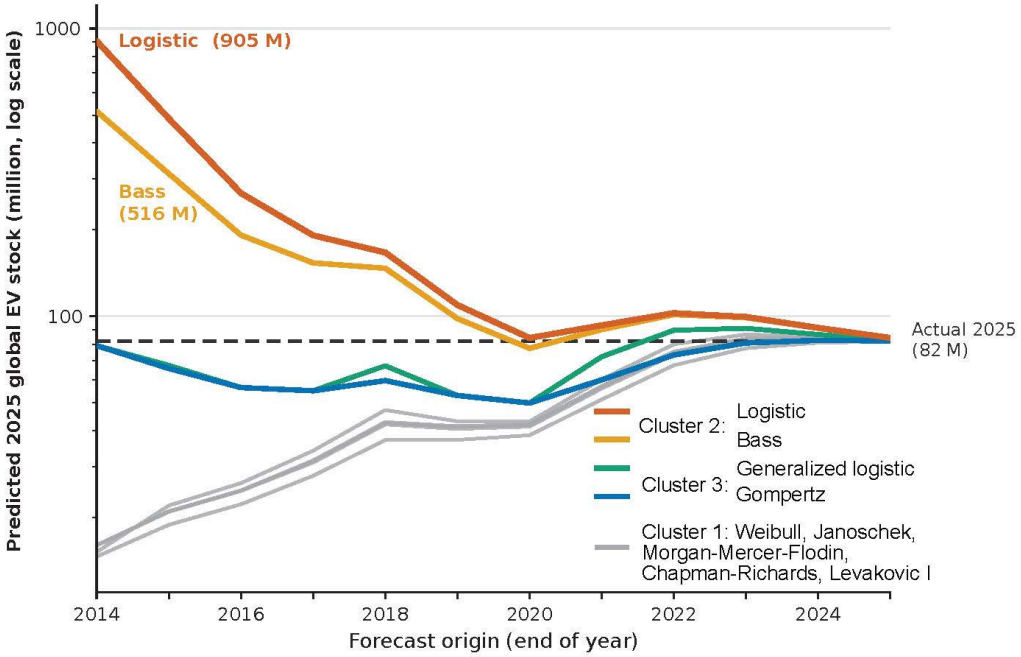


Figure 3. Global stocks for the end of 2025 based on 12 end-of-year projections.

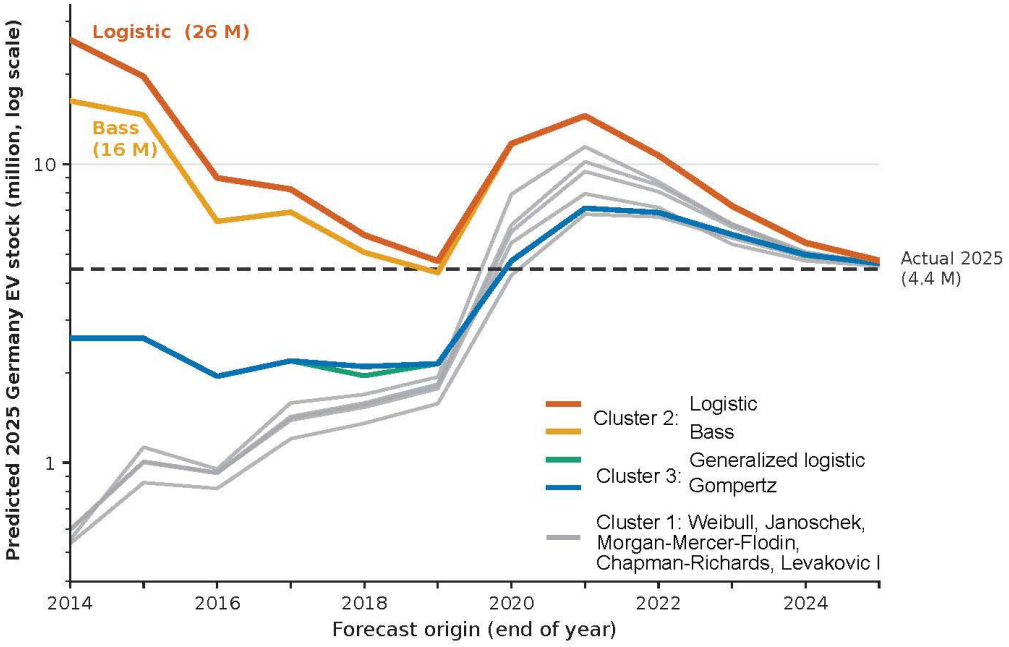


Figure 4. Germany stocks for the end of 2025 based on 12 end-of-year projections.

The predictions of the global inventory figure for 2025 based on data to the end of 2014 using the generalized logistic, Gompertz, and modified Gompertz functions are almost correct (estimated 79 million compared to the actual 82 million). Even though the predictions for the following years are lower, this is a very good result for a 12-year forecast based on only 5 years of historical data. The 2014 forecast for Germany is not as good at 2.6 million compared with the actual 4.4 million (Figure 4).

The forecasts in Figure 5 correspond to the data in Appendix A.3 (global) in accordance with the forecasts made at the end of each year from 2014 to 2025. At the beginning of the data series, the heavy underpredictions of the first cluster and overpredictions of the second cluster are striking. These corresponded to the late years of the inflection point in Cluster 1 and the very early years in Cluster 2. An indication of the steepness of the Bass and logistic functions in Cluster 2 is the short intervals between the point of greatest acceleration and the inflection point (only two to three years). In Cluster 3 (generalized logistic, Gompertz, and modified Gompertz), this interval is approximately 10 years, which seems more realistic for the EV market.

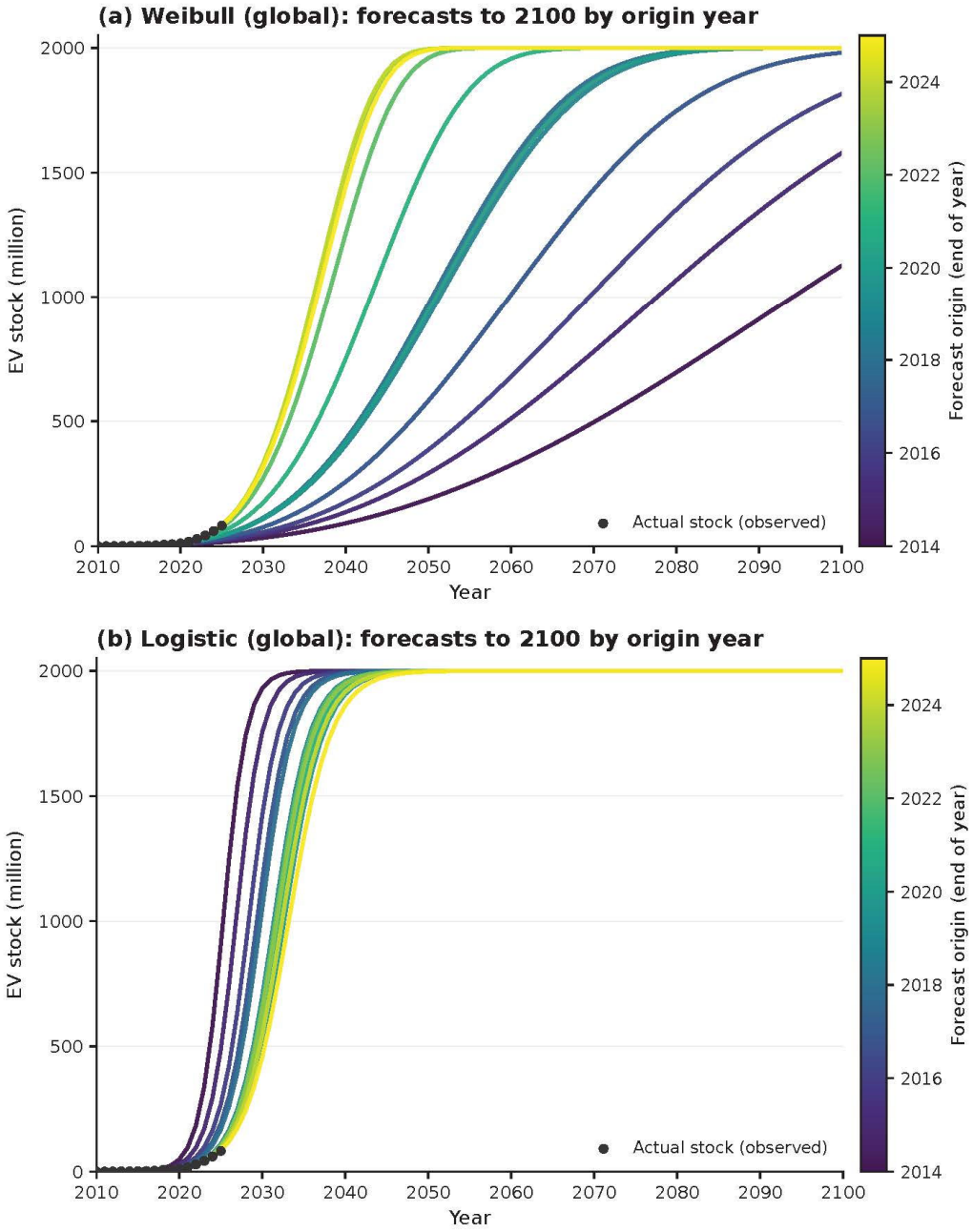


Figure 5. *Cont.*

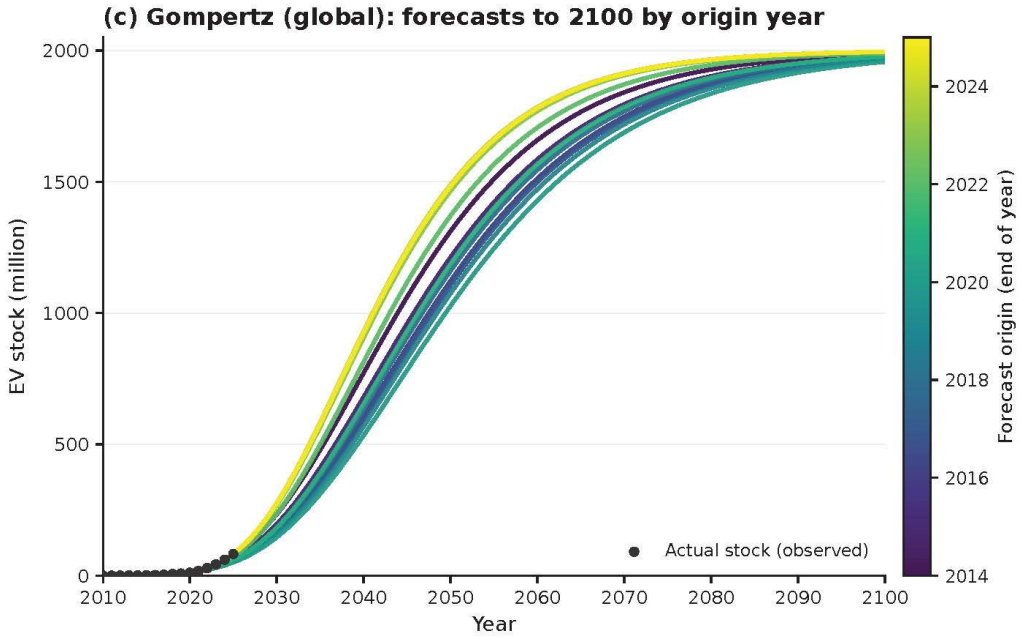


Figure 5. Growth functions for forecasts as of the end of 2014 until 2025.

As expected, the functions in Cluster 1 exhibit the greatest dispersion. The functions in Cluster 2 (logistic, Bass), with the lowest standard deviations, would be preferable; however, their inflection points appear very early because these two functions tend to experience a rapid, steep increase after only about 10 to 15 years from the initial measurement. The poor fit indices thus stem primarily from the earlier forecasts from 2014 onward, with very high forecasts for 2025. Therefore, the functions in Cluster 3 are preferred; although they have slightly higher SDs, their inflection points are shifted by approximately 5 to 10 years later relative to the Bass and logistic functions, making their predictions more conservative.

4.2. Fit Indices

The quality of the growth functions was measured using the three fit indices, *RMSE*, *AIC*, and *MAPE*, over two periods. In the adaption process historical data were used to determine parameters that aligned the function with the actual data; then, the forecast process was applied. In this study, we proceeded as if we already knew the future by taking a retrograde approach (e.g., as if we were at the end of 2014). Using the figures available up to that point from 2010 onwards, the parameters of the growth function (adaptation period) were determined to predict for the years 2015 to 2025. Since the figures up to 2025 were known, the forecast quality could be assessed using the fit indices.

The indices were calculated using Equations (1), (2) and (4) separately for the adaptation and prediction periods for all 10 growth functions. The results are shown in Table 6a for the worldwide data and in Table 6b for Germany.

The *MAPE* values, as a result of being sensitive to small numbers because of small denominators [56], increased unnaturally rapidly at the beginning. For the worldwide figures, this means that for the logistic function in 2010, the *MAPE* was $|\text{actual} - \text{predicted}|/\text{actual} = |6.5 - 44.51|/6.5 = 589\%$. Thus, to reduce distortions in the assessment of the forecast quality, the first two years were excluded from the calculation of the error terms for all functions.

The disadvantages of the *RMSE* and *AIC* are apparent: they could not be compared across two samples with different scales, only within the world and Germany data. The *MAPE* is better in this respect, as it measures scale-independent percentage errors. The *MAPE*s were larger for the German indices, which is not surprising given the unstable de-

velopment of EV stocks from 2020 onwards (Figure 2). However, the judgment for Germany favors the growth functions of Cluster 3, which showed the smallest *RMSE*s, *AIC*s, and *MAPE*s in the forecast periods. The *MAPE*s were also the lowest in the adaptation phase.

Due to the wide spread in the curves across the forecast years in Cluster 1 (Figure 5a) and the steep climbs of Cluster 2 (Figure 5b), the functions of Cluster 3 were preferred. This was particularly evident in the prediction process, in which the *RMSE*, *AIC*, and *MAPE* had the lowest values (Table 6a). In the adaptation process, the Janoschek or Bass functions might also be considered, but their fit indices were so poor for the prediction process (especially Bass) that they were ruled out when selecting the most suitable method.

Table 6. Fit indices.

	(a) World	**Adaptation Process**			**Prediction Process**		
	Fit Indices	***RMSE***	***AIC***	***MAPE***	***RMSE***	***AIC***	***MAPE***
Cluster 1	Weibull	548	1584	22.76%	22,720	1519	34.24%
	Janoschek	441	1542	17.33%	22,062	1518	32.95%
	Morgan–Mercer–Flodin	552	1585	22.98%	22,798	1520	34.36%
	Chapman–Richards	704	1635	27.56%	24,245	1528	37.17%
	Levakovic I	572	1595	23.68%	22,905	1522	34.52%
Cluster 2	Bass	564	1590	13.60%	76,702	1680	70.08%
	Logistic	588	1598	20.22%	144,863	1764	124.88%
Cluster 3	Generalized logistic	371	1507	8.09%	9953	1412	15.09%
	Gompertz	536	1579	17.52%	10,746	1421	16.00%
	Modified Gompertz	536	1579	17.52%	10,746	1421	16.00%
	(b) Germany	**Adaptation Process**			**Prediction Process**		
	Fit Indices	***RMSE***	***AIC***	***MAPE***	***RMSE***	***AIC***	***MAPE***
Cluster 1	Weibull	93	1222	30.80%	1863	1189	50.71%
	Janoschek	89	1215	50.35%	1977	1199	51.85%
	Morgan–Mercer–Flodin	90	1215	30.77%	1803	1185	49.96%
	Chapman–Richards	78	1185	34.94%	1678	1175	48.49%
	Levakovic I	66	1155	35.03%	1681	1178	47.81%
Cluster 2	Bass	121	1276	46.55%	3083	1256	54.50%
	Logistic	123	1282	54.58%	4671	1313	80.57%
Cluster 3	Generalized logistic	84	1204	28.24%	1238	1137	34.41%
	Gompertz	84	1202	28.26%	1230	1134	34.27%
	Modified Gompertz	84	1202	28.26%	1230	1134	34.27%

Note: *RMSE*: Root mean square error; *AIC*: Akaike information criterion; *MAPE*: Mean absolute percentage error.

A one-way ANOVA was conducted for the indices in the prediction process, which is more important than the adaptation process. For both the global and German data, the indices for Cluster 2 were highest (i.e., worst), and for Cluster 3 they were best ($p < 0.001$ for the global *AIC* and the German *RMSE* and *AIC*, $p < 0.01$ for the other three indices). A *t*-test comparing Clusters 1 and 3 showed better (lower) indices in Cluster 3 (all $p < 0.001$).

Within Cluster 3, the better indices in the global analysis seemed to support the generalized logistic model (Table 6a). This was mainly due to the adaption process, in which the generalized logistic function followed stock growth more closely than the two Gompertz functions from 2022 onwards. However, the generalized logistic function drew momentum from the strong sales growth in 2021 and 2022. When growth slowed from 2023 onwards, the forecasts normalized again.

While the functions from Cluster 3 deliver good long- and short-term forecasts and perform reasonably well in the medium term, the bass and logistic functions show poor

results at the beginning of the forecasts, i.e., for long time horizons. However, Cluster 2 appears to perform better in the medium term, with forecasts sometimes better than those of the other two clusters. It is unclear, however, over which time horizons this applies. For the global data, the time horizons are 4 to 6 years, and for the German data, they are 6 to 9 years. Therefore, the use of the Cluster 3 functions is still recommended.

5. Discussion, Outlook, Limitations, and Conclusions

5.1. Discussion

In this study, ten growth functions, including the two equivalent Gompertz functions, were assessed in terms of how well they predicted EV market growth. Since this is only possible by comparing the predicted figures with actual figures, a prediction made at the end of 2025 based on historical data from 2010 (16 years) would have to wait until the next few years had passed. However, we can compare a forecast made at the end of any previous year using the data available up to that time to figures known up to 2025. Using this retrograde approach made it possible to assess each function's suitability for predicting EV stock. The *MAPE* fit index proved more informative than the *RMSE* and the *AIC*. The three indices showed strong and significant positive correlations.

An ideal forecasting function would be one that produces consistently similar forecasts over the years and is not misled by minor market movements, making planning easier for policymakers and industry leaders. For example, one would want the forecast for 2050 made today to be almost identical to the one made 10 years from now. Unfortunately, this was not the case for 7 of the 10 functions tested. The functions from Cluster 1 (Weibull, Janoschek, Morgan–Mercer–Flodin, Chapman–Richards, and Levakovic) started out very flat in earlier years, predicting low future values, but model estimates become more stable as additional observations were included; the curves shifted leftward and became steeper (Figure 5a).

The functions in Cluster 2 (logistic and Bass) behaved in the opposite way. With only a few data points, they started steeply with very high values (the global forecast at the end of 2014 predicted a stock of 900 million EVs for 2025, vs. an actual stock of 82 million). As the number of observation points increased, approaching the present, the curves became more realistic, shifting to the right and flattening out (Figure 5b).

The functions in Cluster 3 (generalized logistic, Gompertz, and modified Gompertz) appeared the most suitable for predicting future stock: they were the only ones capable of suitable predictions of the total EV stock at the end of 2025 as early as the end of 2014. Even though their accuracy declined in subsequent years, this was a remarkable achievement. Furthermore, the spread of their annual consecutive forecasts was low (Figure 5c), which is why they were never completely wrong, unlike, for example, the functions from Cluster 1, which showed excessive spreads (Figure 5a).

Of the three functions in Cluster 3, the generalized logistic function had the greatest spread, which is why the Gompertz functions are recommended; both deliver identical results. The modified Gompertz function is more advantageous because the parameters are easier to interpret (the inflection point is determined solely by the parameter β, and the point of maximum acceleration is calculated by adding β and γ multiplied by the scalar –0.96242365).

The realization that specific technologies diffuse along an asymmetric Gompertz trajectory rather than the symmetric logistic is most effectively comprehended as a reflection of the underlying adoption mechanism, rather than a matter of curve-fitting convenience. The logistic function is characterized by a relative growth rate that decreases with the logarithm of penetration, $ln(K/N)$, whereas the Gompertz function is embodied by a relative growth rate that is proportional to the interaction between adopters and non-adopters, $N(K - N)$. Consequently, the logistic function reaches its maximum at half-saturation. This results in

a right-skewed profile, with a rapid early take-off followed by a protracted approach to saturation, because the inflection point is shifted forward to approximately 36.8% of the ceiling. Such asymmetry is consistent with several features common to technological diffusion. First, adopter populations are frequently heterogeneous in a skewed manner, combining a minority of eager early adopters with a long tail of structurally resistant laggards who are progressively costlier to reach, so that the last increments of market penetration accrue only slowly. Second, the deceleration of growth is often governed not by social imitation but by supply side and capability constraints—infrastructure build-out, complementary assets, and learning-by-doing—whose effect is to shrink the "distance to the frontier" multiplicatively; this proportionate-growth logic is precisely what generates Gompertzian dynamics in cognate domains such as organismal and tumor growth, and in the broader analysis of growth equations. Third, the benefits of adoption are frequently front-loaded through network and first-mover advantages, concentrating adoption incentives early in the process. A superior Gompertz fit should be interpreted as evidence consistent with skewed heterogeneity or a decaying internal driving force, rather than as conclusive confirmation of any single generative mechanism. Importantly, the logistic and Gompertz forms only diverge significantly in the upper tail and near the inflection point, where empirical data are frequently sparse.

5.2. Outlook

The purpose of this study was to identify suitable growth functions for the EV market. However, it is advisable to mention additional findings that came to light in the process. It should be noted that we do not call these forecasts due to the long time horizons, until 2050 or even 2100, framing them instead as illustrative scenarios.

As shown in Figure 6, based on extrapolation using the Gompertz function, the EV market in Germany is expected to reach 86% saturation by the end of 2050, and 74% worldwide (These forecasts are likely too high because scrapping was not considered. If annual scrapping of 1.5% of the vehicle stock were factored in, the EV share in 2050 would be only 62% instead of 74%). This means that the zero-carbon target cannot be achieved by then with EVs alone. However, this only applies if other parameters do not change: fleet turnover, electricity generation, travel demand, and non-EV modes.

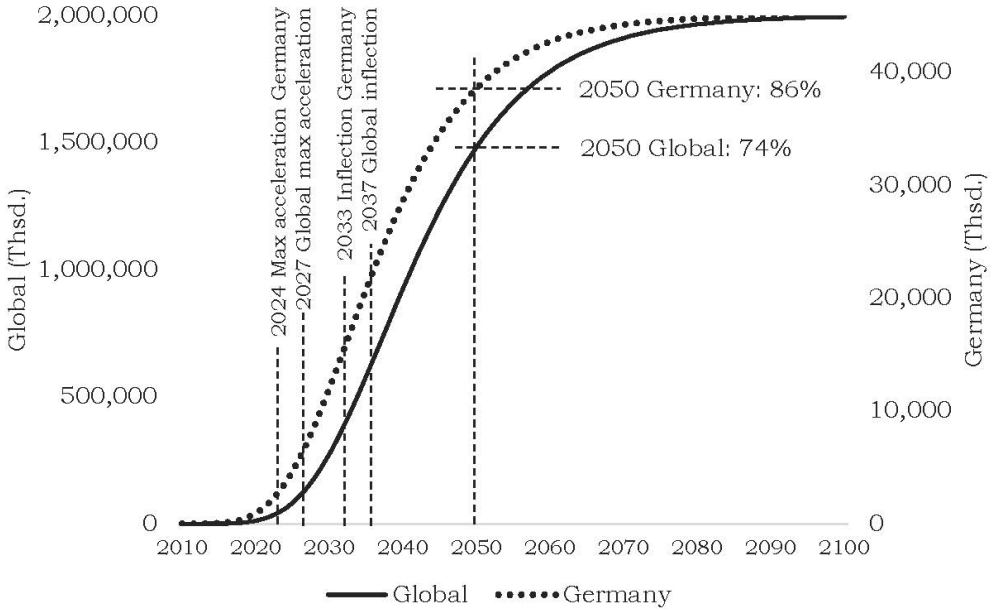


Figure 6. Stocks until 2100 predicted with the Gompertz function as of the end of 2025.

Nevertheless, there is no reason for pessimism. While the inflection point where sales peak will not be reached for another 10 years or more, the point of maximum acceleration is not far off (2027 worldwide; in Germany, it was reached in 2024).

The maximum acceleration is also important. Before this point (A in Figure 1), the curve is accelerating and still rising ($f'' > 0$, $f''' > 0$): the "throttle opening" build-up. After the maximum acceleration point, the curve is still accelerating, but acceleration is now falling ($f'' > 0$, $f''' < 0$): the steepest, most exponential-looking stretch, ending at maximum growth, which is the inflection point (B in Figure 1).

The point of maximum acceleration lies in a period that Moore (1991) [57] refers to as "the chasm" (Brdulak et al., 2021 [38]; Rogers, 2003 [39]). This point is important for manufacturers because, after the introduction phase, in which innovators and early adopters are the first customers, the mass market is reached beyond this chasm. Thus, reaching maximum acceleration signals that the chasm is about to be crossed.

5.3. Limitations

The results can only be applied to the electric vehicle market. It is not even certain that the findings are applicable to the entire passenger car market. Further research is needed to clarify this.

As with any prediction, these results should be viewed with caution. The method used here has the following limitations. Not all growth functions could be included, as this would go beyond the scope of this study. Nevertheless, it was possible to examine nine functions grouped into three clusters. However, the application of some of these functions to electromobility may be limited, and they may be better suited to biology, botany, or medicine, because the growth of bacteria and body cells is different to that of innovative car markets.

Confidence intervals for the model parameters were generated by SPSS but not recorded; only the parameter values themselves were noted. An examination using the Gompertz model yielded very low standard errors: approximately 0.095 for coefficient *b* (with a value of ~12–14) and 0.001 for *c* (with a value of 0.075, i.e., around 1%). Given their limited relevance to the specific research question, we decided not to report them. Confidence intervals for the growth curve and prediction intervals cannot be directly extracted from SPSS, nor are they critical to the analysis.

The saturation limit was set at the same level for all functions, but this estimate might be too low. Forecasts for the total passenger car market up to 2050 range from 2.5 billion to over 3 billion vehicles (Prospects 2050, 2025 [48]); however, it is not yet known whether the entire vehicle fleet will be electric by then. For this reason, the saturation limit was set at 2 billion worldwide and 45 million in Germany. To analyze the effects of different limits, calculations were performed for each of the three cluster models with limits of 1.5 and 3 billion EVs. These demonstrated the robustness of the functions: the parameters for the growth rate (k for Weibull, r for logistic, and c for Gompertz) remained almost identical; only the shape parameters increased from the 1.5 bn sample to the 3 bn sample, meaning the inflection points shifted slightly to the right in the future, but only for the Weibull and Gompertz functions; for the logistic function, the inflection points remained almost constant. As Table 7 shows, there are only slight differences whether using a limit of 1.5, 2, or 3 billion.

For the important *MAPE* index, a *t*-test for the Gompertz data showed no significant differences (between 1.5 and 2 bn: $p = 0.098$, between 1.5 and 3 bn: $p = 0.489$, between 2 bn and 3 bn: $p = 0.770$; not significant). We assume that the slight changes occur for all functions in the same direction and thus the differences do not influence the decision-making process regarding the most suitable model.

The sample designated "World" or "Global" included all countries with available EV sales figures; however, this accounts for only 85% of the world's population, so in 2050, only 63% saturation will be achieved worldwide (74% × 85%). No EV sales figures are available for many African countries.

Table 7. Fit indices for three functions with saturation limits of 2 and 3 billion EVs.

	Adaptation			Prediction		
Fit Indices	***RMSE***	***AIC***	***MAPE***	***RMSE***	***AIC***	***MAPE***
Weibull 1.5 bn	549	1584	22.84%	22,747	1520	34.28%
Weibull 2 bn	548	1584	22.76%	22,720	1519	34.24%
Weibull 3 bn	547	1583	22.69%	22,694	1519	34.20%
Logistic 1.5 bn	575	1594	19.81%	129,013	1749	118.06%
Logistic 2 bn	588	1598	20.22%	144,863	1764	124.88%
Logistic 3 bn	601	1603	20.62%	165,626	1782	133.04%
Gompertz 1.5 bn	565	1590	18.46%	11,642	1431	16.62%
Gompertz 2 bn	536	1579	17.52%	10,746	1421	16.00%
Gompertz 3 bn	505	1567	16.28%	9732	1407	15.72%

Note: *RMSE*: root mean square error; *AIC*: Akaike information criterion; *MAPE*: mean absolute percentage error.

5.4. Conclusions

This study evaluated a set of ten sigmoid growth functions for retrospectively forecasting EV stock. The results are conditional on the EV Volumes data source, on cumulative registrations as a proxy for stock, on externally fixed saturation levels, and on the expanding-window retrospective design. Within these conditions, Gompertz-type functions appear the most promising for stable long-horizon forecasting; the generalized logistic performs comparably—indeed, marginally better on global point accuracy—and should not be dismissed. Future research should benchmark these growth curves against time-series and hybrid models that incorporate policy and market drivers, and against endogenously estimated saturation levels.

Supplementary Materials: The following supporting information can be downloaded at: https://www.mdpi.com/article/10.3390/wevj17080385/s1, Growth Functions World.xlsx; Growth Functions Germany.xlsx.

Funding: This research received no external funding.

Data Availability Statement: The original contributions presented in this study are included in the article/Supplementary Materials. Further inquiries can be directed to the corresponding author.

Acknowledgments: During the preparation of this work, the author used artificial intelligence tools such as ChatGPT (5.6 Sol) and Claude (Open 4.8) to clarify the theoretical background of growth functions, their derivatives, and roots, as well as certain formulations. After using this tool, the author reviewed and edited the content as needed and takes full responsibility for the published article. The literature review was performed by the author; the table, however, was compiled by Claude and double-checked by ChatGPT and the author.

Conflicts of Interest: The author declares no conflicts of interest.

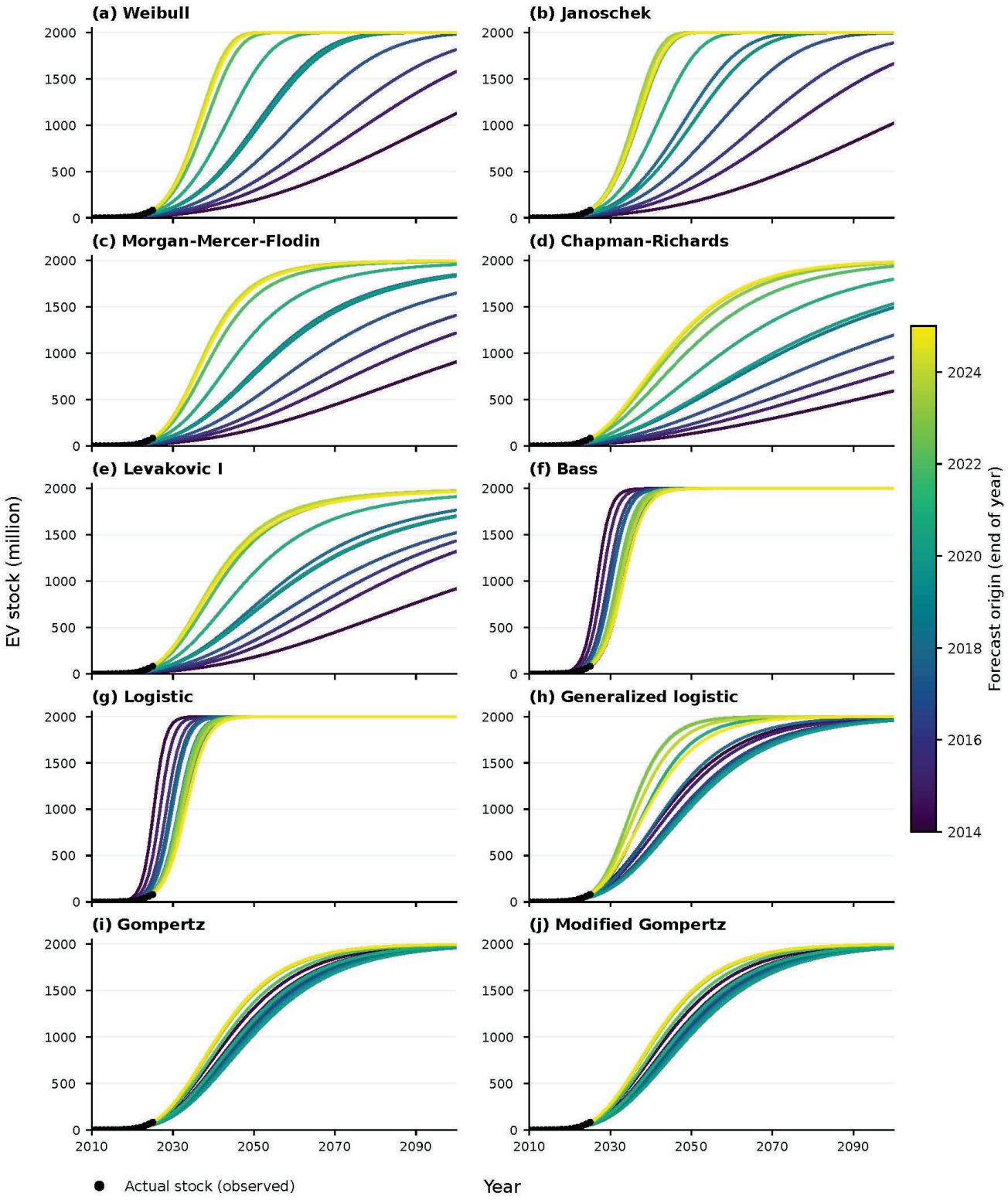
Abbreviations

The following abbreviations are used in this manuscript:

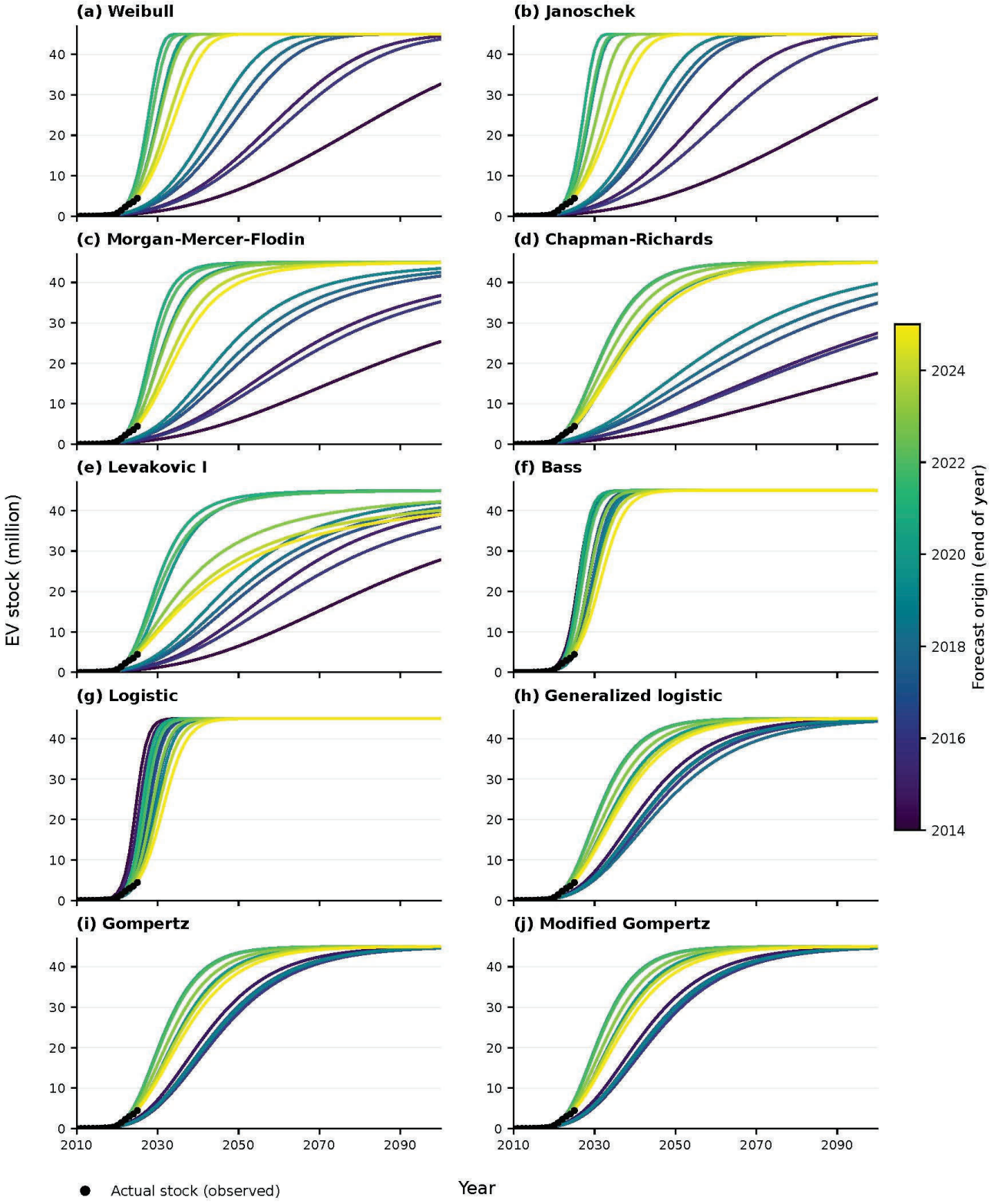
RMSE	Root mean square error
AIC	Akaike information criterion
MAPE	Mean absolute percentage error

Appendix A

Appendix A.1. Global: Forecasts of EV Stock to 2100 by Model and Forecast Origin



Appendix A.2. Germany: Forecasts of EV Stock to 2100 by Model and Forecast Origin



Appendix A.3. Global: Inventory Forecasts for 2025, Inflection and Maximum Acceleration Points for Forecasts from 2014 to 2025

Table A1. Global-forecast of 2025 EV stock (thousand), inflection year, and maximum-acceleration year, by growth model and forecast origin (end of year). Within each column (forecast origin), bold marks every model whose 2025 forecast lies within ±5% of the best (closest-to-observed) forecast in that column (observed value 81,973 thousand); several models may qualify, and a given model may be highlighted in several columns, one, or none. Cluster 3 models (Gompertz family) are set in bold in the first column.

Model	2014	2015	2016	2017	2018	2019	2020	2021	2022	2023	2024	2025	Actual Stock 2025
Forecast of 2025 EV stock (thousand)													
Weibull	16,020	20,997	24,821	31,540	42,901	41,494	42,149	57,154	75,404	**83,784**	**84,226**	**82,513**	**81,973**
Janoschek	15,164	21,983	26,305	34,083	47,230	43,125	43,066	60,337	**79,917**	86,441	**85,131**	**82,667**	**81,973**
Morgan-Mercer-Flodin	15,964	20,904	24,698	31,350	42,565	41,218	41,903	56,729	74,760	**83,204**	**83,901**	**82,442**	**81,973**
Chapman-Richards	14,613	18,840	22,214	27,884	37,125	37,180	38,582	51,359	67,540	77,395	**80,863**	**81,664**	**81,973**
Levakovic I	15,977	21,000	24,733	31,012	42,052	40,576	41,317	56,060	73,536	**81,810**	**83,090**	**82,242**	**81,973**
1-14 Bass	515,569	312,966	191,415	153,260	146,815	**98,166**	77,396	**89,871**	101,331	98,900	90,867	**83,968**	**81,973**
Logistic	904,660	486,706	267,815	191,020	166,577	109,436	**84,062**	**93,021**	102,573	99,491	91,185	**84,088**	**81,973**
Generalized logistic	**79,069**	**67,487**	**56,525**	**55,097**	**67,270**	53,056	49,942	72,326	89,404	90,821	**86,402**	**82,612**	**81,973**
Gompertz	**79,042**	**65,846**	**56,505**	**55,083**	59,752	53,045	49,939	60,092	73,372	**80,755**	**82,498**	**82,123**	**81,973**
Modified Gompertz	**79,042**	**65,846**	**56,505**	**55,083**	59,752	53,045	49,939	60,092	73,372	**80,755**	**82,498**	**82,123**	**81,973**
Year of inflection point													
Weibull	2091	2076	2069	2060	2051	2052	2051	2044	2039	2037	2037	2037	
Janoschek	2095	2074	2066	2057	2048	2050	2051	2042	2037	2036	2036	2037	
Morgan-Mercer-Flodin	2082	2070	2063	2056	2048	2049	2049	2042	2037	2036	2036	2036	
Chapman-Richards	2098	2084	2076	2066	2057	2057	2056	2048	2042	2039	2038	2038	
Levakovic I	2082	2070	2063	2056	2049	2049	2049	2042	2038	2036	2036	2036	
1-14 Bass	2027	2028	2029	2030	2030	2032	2033	2032	2032	2032	2032	2033	
Logistic	2025	2027	2028	2029	2030	2031	2033	2032	2032	2032	2032	2033	
1-14 Generalized logistic	2039	2041	2042	2043	2040	2043	2044	2037	2034	2034	2035	2036	
Gompertz	2039	2041	2042	2043	2042	2043	2044	2041	2039	2037	2037	2037	
Modified Gompertz	2039	2041	2042	2043	2042	2043	2044	2041	2039	2037	2037	2037	
Year of maximum acceleration													
1-14 Weibull	2048	2045	2043	2040	2037	2037	2037	2034	2032	2031	2031	2031	
Janoschek	2049	2044	2042	2039	2036	2037	2037	2033	2031	2031	2031	2031	
Morgan-Mercer-Flodin	2040	2038	2037	2035	2033	2033	2033	2031	2029	2029	2029	2029	
Chapman-Richards	2029	2029	2029	2029	2028	2028	2028	2027	2027	2026	2026	2026	
Levakovic I	2041	2040	2037	2033	2032	2031	2031	2030	2029	2028	2028	2027	
Bass	2025	2026	2027	2027	2028	2029	2030	2029	2029	2029	2029	2030	
Logistic	2023	2025	2026	2027	2027	2028	2029	2029	2029	2029	2029	2030	
Generalized logistic	2028	2028	2029	2029	2029	2030	2030	2029	2028	2028	2028	2028	
Gompertz	2028	2028	2029	2029	2029	2030	2030	2029	2028	2027	2027	2027	
Modified Gompertz	2028	2028	2029	2029	2029	2030	2030	2029	2028	2027	2027	2027	

Models grouped by cluster: Cluster 1 (Weibull, Janoschek, Morgan–Mercer–Flodin, Chapman–Richards, Levakovic I), Cluster 2 (Bass, Logistic), Cluster 3 (Generalized logistic, Gompertz, Modified Gompertz).

Appendix A.4. Germany: Inventory Forecasts for 2025, Inflection and Maximum Acceleration Points for Forecasts from 2014 to 2025

Table A2. Germany-forecast of 2025 EV stock (thousand), inflection year, and maximum-acceleration year, by growth model and forecast origin (end of year). Within each column (forecast origin), bold marks every model whose 2025 forecast lies within ±5% of the best (closest-to-observed) forecast in that column (observed value 4442 thousand); several models may qualify, and a given model may be highlighted in several columns, one, or none.

Model	2014	2015	2016	2017	2018	2019	2020	2021	2022	2023	2024	2025	Actual Stock 2025
Forecast of 2025 EV stock (thousand)													
1-14 Weibull	597	1010	928	1427	1584	1832	6254	10,186	8497	6302	5073	**4647**	**4442**
Janoschek	551	1126	951	1585	1692	1936	7928	11,425	8726	6279	5033	**4630**	**4442**
Morgan-Mercer-Flodin	593	1001	920	1410	1564	1807	5944	9445	8088	6160	5029	**4639**	**4442**
Chapman-Richards	535	857	819	1202	1354	1576	**4240**	**6790**	**6656**	**5653**	**4880**	**4606**	**4442**
Levakovic I	597	1010	923	1387	1534	1770	5455	7954	7148	**5390**	**4743**	**4560**	**4442**
1-14 Bass	16,285	14,616	**6428**	6904	**5061**	**4329**	11,672	14,498	10,665	7217	5420	**4736**	**4442**
Logistic	26,077	19,643	8987	8237	5788	4735	11,709	14,506	10,687	7253	5457	**4756**	**4442**
Generalized logistic	**2611**	**2612**	1946	**2192**	1953	2145	4739	**7117**	**6883**	5810	**4946**	**4667**	**4442**
Gompertz	**2611**	**2611**	1945	**2193**	2098	2146	4739	**7117**	**6883**	5808	**4973**	**4644**	**4442**
Modified Gompertz	**2611**	**2611**	1945	**2193**	2098	2146	4739	**7117**	**6883**	5808	**4973**	**4644**	**4442**
Year of inflection point													
1-14 Weibull	2078	2058	2060	2049	2046	2043	2030	2028	2029	2031	2033	2034	
Janoschek	2083	2054	2059	2046	2045	2042	2029	2027	2029	2031	2033	2034	
Morgan-Mercer-Flodin	2070	2053	2056	2046	2044	2041	2030	2027	2028	2030	2031	2032	
Chapman-Richards	2083	2063	2065	2053	2050	2047	2033	2029	2029	2031	2032	2033	
Levakovic I	2070	2053	2056	2046	2044	2041	2030	2028	2028	2029	2029	2030	
1-14 Bass	2026	2026	2029	2028	2029	2030	2027	2026	2027	2029	2030	2031	
Logistic	2025	2025	2028	2028	2029	2030	2027	2026	2027	2028	2030	2031	
1-14 Generalized logistic	2037	2037	2040	2039	2041	2039	2032	2029	2029	2030	2032	2033	
Gompertz	2037	2037	2040	2039	2039	2039	2032	2029	2029	2030	2032	2033	
Modified Gompertz	2037	2037	2040	2039	2039	2039	2032	2029	2029	2030	2032	2033	
Year of maximum acceleration													
1-14 Weibull	2048	2042	2043	2038	2037	2036	2028	2027	2027	2028	2029	2030	
Janoschek	2042	2036	2037	2033	2033	2032	2026	2025	2025	2026	2027	2027	
Morgan-Mercer-Flodin	2034	2032	2032	2030	2030	2029	2025	2024	2024	2025	2025	2025	
Chapman-Richards	2025	2026	2026	2025	2025	2025	2023	2022	2023	2023	2023	2023	
Levakovic I	2037	2033	2033	2029	2028	2028	2024	2023	2023	2021	2021	2020	
Bass	2024	2024	2026	2026	2027	2027	2025	2024	2025	2026	2027	2027	
Logistic	2023	2023	2025	2025	2026	2027	2025	2024	2025	2026	2027	2027	
Generalized logistic	2026	2026	2027	2027	2027	2027	2024	2023	2023	2023	2024	2024	
Gompertz	2026	2026	2027	2027	2027	2027	2024	2023	2023	2023	2024	2024	
Modified Gompertz	2026	2026	2027	2027	2027	2027	2024	2023	2023	2023	2024	2024	

Models grouped by cluster as in Table A1.

References

1. United Nations Economic Commission for Europe. Electric Vehicles and Their Potential to Realize the Sustainable Development Agenda. In *Electrification of Mobility*; United Nations iLibrary: New York, NY, USA, 2025. Available online: https://www.un-ilibrary.org/content/books/9789211066883c007 (accessed on 20 July 2026).
2. EV-Volumes. Available online: https://ev-volumes.com/ (accessed on 20 July 2026).
3. United Nations. Paris Agreement. Available online: https://unfccc.int/process-and-meetings/the-paris-agreement (accessed on 20 July 2026).
4. IEA International Energy Agency. *Net Zero Roadmap: A Global Pathway to Keep the 1.5 °C Goal in Reach*; IEA International Energy Agency: Paris, France, 2023; pp. 1–226. Available online: https://www.iea.org/reports/net-zero-roadmap-a-global-pathway-to-keep-the-15-0c-goal-in-reach (accessed on 20 July 2026).
5. Shamsuddoha, M.; Tasnuba, N. The Road Ahead for Hybrid or Electric Vehicles in Developing Countries: Market Growth, Infrastructure, and Policy Needs. *World Electr. Veh. J.* **2025**, *16*, 180. [CrossRef]
6. Han, G.; Li, Z. A Structured Review of Electric Vehicle Sales Research: Multi-Level Driving Factors and Forecasting Pathways over the Past Decade. *World Electr. Veh. J.* **2026**, *17*, 122. [CrossRef]
7. Lieven, T.; Mühlmeier, S.; Henkel, S.; Waller, J.F. Who will buy electric cars? An empirical study in Germany. *Transp. Res. Part D Transp. Environ.* **2011**, *16*, 236–243. [CrossRef]
8. Sierzchula, W.; Bakker, S.; Maat, K.; Van Wee, B. The influence of financial incentives and other socio-economic factors on electric vehicle adoption. *Energy Policy* **2014**, *68*, 183–194. [CrossRef]
9. Srinivasan, B. Predicting Future Electric Vehicle (EV) Sales: A Time Series Forecasting Approach Using Historical EV Sales Data. *Int. J. Appl. Inf. Manag.* **2025**, *5*, 177–189. [CrossRef]
10. Malthus, T.R. *An Essay on the Principle of Population, as It Affects the Future Improvement of Society*; J. Johnson: London, UK, 1789.
11. Rietmann, N.; Hügler, B.; Lieven, T. Forecasting the trajectory of electric vehicle sales and the consequences for worldwide CO_2 emissions. *J. Clean. Prod.* **2020**, *261*, 121038. [CrossRef]
12. Zeide, B. Analysis of Growth Equations. *For. Sci.* **1993**, *39*, 594–616. [CrossRef]
13. Goriely, A. The Mathematics and Mechanics of Biological Growth. In *Interdisciplinary Applied Mathematics*; Springer: Berlin/Heidelberg, Germany, 2017; Volume 45.
14. Monod, J. The Growth of Bacterial Cultures. *Annu. Rev. Microbiol.* **1949**, *3*, 371–394. [CrossRef]
15. West, B.; Brown, J.H.; Enquist, B.J. A General Model for the Origin of Allometric Scaling Laws in Biology. *Science* **1997**, *276*, 122–126. [CrossRef] [PubMed]
16. Murray, J.D. *Mathematical Biology I: An Introduction*, 3rd ed.; Springer: Berlin/Heidelberg, Germany, 2002.
17. Murray, J.D. *Mathematical Biology II: Spatial Models and Biomedical Applications*, 3rd ed.; Springer: Berlin/Heidelberg, Germany, 2003.
18. Hunt, R. *Plant Growth Curves: The Functional Approach to Plant Growth Analysis*; Edward Arnold: London, UK, 1982.
19. Hunt, R. *Basic Growth Analysis: Plant Growth Analysis for Beginners*; Unwin Hyman: London, UK, 1990.
20. Evans, L.T. *The Quantitative Analysis of Plant Growth*; University of California Press: Oakland, CA, USA, 1972.
21. Kermack, W.O.; McKendrick, A.G. A Contribution to the Mathematical Theory of Epidemics. *Proc. R. Soc. A* **1927**, *115*, 700–721. [CrossRef]
22. Keeling, M.J.; Rohani, P. *Modeling Infectious Diseases in Humans and Animals*; Princeton University Press: Princeton, NJ, USA, 2008.
23. Viboud, C.; Simonsen, L.; Chowell, G. A Generalized-Growth Model to Characterize the Early Ascending Phase of Infectious Disease Outbreaks. *Epidemics* **2016**, *15*, 27–37. [CrossRef] [PubMed]
24. Laird, A.K. Dynamics of Tumour Growth. *Br. J. Cancer* **1964**, *18*, 490–502. [CrossRef] [PubMed]
25. Solow, R.M. A Contribution to the Theory of Economic Growth. *Q. J. Econ.* **1956**, *70*, 65–94. [CrossRef]
26. Swan, T.W. Economic Growth and Capital Accumulation. *Econ. Rec.* **1956**, *32*, 334–361. [CrossRef]
27. Barro; R.J. Sala-i-Martin, X. *Economic Growth*; McGraw-Hill: Columbus, OH, USA, 1995.
28. Mankiw, N.G.; Romer, D.; Weil, D.N. A Contribution to the Empirics of Economic Growth. *Q. J. Econ.* **1992**, *107*, 407–437. [CrossRef]
29. Gompertz, B. XXIV. On the nature of the function expressive of the law of human mortality, and on a new mode of determining the value of life contingencies. *Philos. Trans. R. Soc. Lond.* **1825**, *115*, 513–583. [CrossRef]
30. Verhulst, P.F. Notice sur la loi que la population poursuit dans son accroissement. *Corresp. Mathématique Phys.* **1838**, *10*, 113–121.
31. Bacaër, N. Verhulst and the logistic equation (1838). In *A Short History of Mathematical Population Dynamics*; Springer: London, UK, 2011; pp. 35–39. [CrossRef]
32. Richards, J. A Flexible Growth Function for Empirical Use. *J. Exp. Bot.* **1959**, *10*, 290–301. [CrossRef]
33. Tjørve, E.; Tjørve, K.M.C. A Unified Approach to the Richards Model Family for Use in Growth Analyses. *J. Theor. Biol.* **2010**, *267*, 417–425. [CrossRef] [PubMed]
34. Tjørve, K.M.C.; Tjørve, E. The use of Gompertz models in growth analyses, and new Gompertz-model approach: An addition to the Unified-Richards family. *PLoS ONE* **2017**, *12*, e0178691. [CrossRef] [PubMed]
35. Young, P. Technological growth curves. A competition of forecasting models. *Technol. Forecast. Soc. Change* **1993**, *44*, 375–389. [CrossRef]

36. Buchanan, R.L.; Whiting, R.C.; Damert, W.C. When is simple good enough: A comparison of the Gompertz, Baranyi, and three-phase linear models for fitting bacterial growth curves. *Food Microbiol.* **1997**, *14*, 313–326. [CrossRef]
37. Huo, H.; Wang, M. Modeling future vehicle sales and stock in China. *Energy Policy* **2012**, *43*, 17–29. [CrossRef]
38. Brdulak, A.; Chaberek, G.; Jagodziński, J. BASS Model Analysis in "Crossing the Chasm" in E-Cars Innovation Diffusion Scenarios. *Energies* **2021**, *14*, 3216. [CrossRef]
39. Rogers, E.M. *Diffusion of Innovations*, 5th ed.; Free Press: New York, NY, USA, 2003.
40. Fan, H.; Li, Z.; Duan, Y.; Wang, B. Incentive policy formulation for China's electric vehicle market: Navigating pathways to sustainable mobility with a green premium analytical model. *Energy Policy* **2025**, *202*, 114610. [CrossRef]
41. Alatawneh, A.; Ghunaim, D. Towards vehicle electrification: A mathematical prediction of battery electric vehicle ownership growth, the case of Turkey. *Green Energy Intell. Transp.* **2024**, *3*, 100166. [CrossRef]
42. Ayyadi, S.; Maaroufi, M. Diffusion models for predicting electric vehicles market in Morocco. In *Proceedings of the 2018 International Conference and Exposition on Electrical And Power Engineering (EPE), Iasi, Romania, 18–19 October 2018*; IEEE: New York, NY, USA, 2018. [CrossRef]
43. Dalkic-Melek, G.; Saltik, E.C.; Tuydes-Yaman, H. Electric Vehicle (EV) Market Penetration in Countries with Rising Motorization Rates. *Int. J. Civ. Eng.* **2025**, *23*, 461–480. [CrossRef]
44. Tang, B.J.; Wu, X.F.; Zhang, X. Modeling the CO_2 emissions and energy saved from new energy vehicles based on the logistic-curve. *Energy Policy* **2013**, *57*, 30–35. [CrossRef]
45. Kumar, R.; Guha, P.; Chakraborty, A. Comparative assessment and selection of electric vehicle diffusion models: A global outlook. *Energy* **2022**, *238*, 121932. [CrossRef]
46. Kraftfahrt-Bundesamt (KBA) Germany. Monatliche Neuzulassungen (Monthly New Registrations). Available online: https://www.kba.de/DE/Statistik/Fahrzeuge/Neuzulassungen/MonatlicheNeuzulassungen/monatl_neuzulassungen_node.html (accessed on 31 December 2024).
47. Lewis, C.D. *Industrial and Business Forecasting Methods: A Practical Guide to Exponential Smoothing and Curve Fitting*; Butterworth-Heinemann: Oxford, UK, 1982.
48. Prospects 2050. World Vehicle Forecasts & Strategies Propects 2050. 2025. Available online: https://prospects-2050.com/wp-content/uploads/2025/04/World-Global-Prospects-2050.pdf (accessed on 20 July 2026).
49. Weibull, W. A statistical distribution function of wide applicability. *J. Appl. Mech.* **1951**, *18*, 293–297. [CrossRef]
50. Janoschek, A. Das reaktionskinetische Grundgesetz und seine Beziehungen zum Wachstums- und Ertragsgesetz. *Stat. Vierteljahresschr.* **1957**, *10*, 25–37.
51. Morgan, P.H.; Mercer, L.P.; Flodin, N.W. General Model for Nutritional Responses of Higher Organisms. *Proc. Natl. Acad. Sci. USA* **1975**, *72*, 4327–4331. [CrossRef] [PubMed]
52. Levakovic, A. Analitički oblik zakona rastenja (Analytical form of the laws of growth). *Glas. Za Šumske Pokuse* **1935**, *4*, 189–282.
53. Bass, F.M. A New Product Growth Model for Consumer Durables. *Manag. Sci.* **1969**, *15*, 215–227. [CrossRef]
54. Tsoularis, A.; Wallace, J. Analysis of Logistic Growth Models. *Math. Biosci.* **2002**, *179*, 21–55. [CrossRef] [PubMed]
55. Dargay, J.; Gately, D.; Sommer, M. Vehicle Ownership and Income Growth, Worldwide: 1960–2030. *Energy J.* **2007**, *28*, 143–170. [CrossRef]
56. Tofallis, C. A better measure of relative prediction accuracy for model selection and model estimation. *J. Oper. Res. Soc.* **2021**, *66*, 1352–1362.
57. Moore, G.A. *Crossing the Chasm: Marketing and Selling Disruptive Products to Mainstream Customers*; Harper Business Essentials: New York, NY, USA, 1991.

Disclaimer/Publisher's Note: The statements, opinions and data contained in all publications are solely those of the individual author(s) and contributor(s) and not of MDPI and/or the editor(s). MDPI and/or the editor(s) disclaim responsibility for any injury to people or property resulting from any ideas, methods, instructions or products referred to in the content.